Control of SPP propagation and focusing through scattering from nanostructures

P.N. Melentiev, A.A. Kuzin, V.I. Balykin

Abstract. **Measuring the characteristics of radiation scattered by surface plasmon polariton waves and detecting them in the far field is the only efficient method for studying the directivity of propagation, wave vector magnitude, and propagation length of such waves. In the present work, we demonstrate that it is possible to control the properties of surface plasmon polaritons propagating along the surface of metal nanofilms by scattering from nanoobjects, namely, nanogrooves and nanopits, formed in the nanofilms. It is shown that this technique allows the main parameters of surface plasmon polaritons to be measured.**

1. Introduction

Surface plasmon polaritons (SPPs) are oscillations in the optical frequency range of free metal electrons at a metal–dielectric interface [1–4]. Great interest in the development of the excitation, control, and detection of such waves is associated with the possibility of using them as information carriers because SPPs combine the advantages of electrons (the possibility of strong spatial localisation) and photons (high oscillation frequency) [5, 6]. To date, various elements of plasmon optics have already been implemented: plasmon mirrors [7, 8], plasmon beam splitters [9], waveguides [10], interferometers [11, 12], lenses [13, 14], and sensors [15–18].

The optics of plasmon polaritons includes the following main components: SPP propagation medium, SPP source, SPP optical elements (lenses, mirrors, etc.), and SPP detection devices. All these elements of plasmon optics are interconnected; therefore, any significant improvement in any of them without the development of other elements is impossible.

There are many studies dedicated to the search for optimal media for the propagation of SPPs [19–22]. An optimal medium exhibits the lowest SPP losses, minimal ohmic losses, and no scattering losses associated with the presence of surface and volumetric inhomogeneities in nanofilms. This ensures the possibility of achieving the longest SPP propagation length. The best results of SPP excitation and propagation were obtained using single-crystal films of gold and silver [12, 23, 24].

A big problem in the optics of SPPs is measuring their propagation parameters. The most advanced research method is near-field microscopy [25, 26]. In this method, a probe of a near-field microscope is placed in the SPP field so that the field scattered by the probe is recorded in the far field. The near field of a SPP can be characterised in terms of the measured dependence of the wave amplitude in the far field and its polarisation depending on the position of the microscope probe [27]. The main problems of this method are the need to possess an expensive device (a near-field microscope) at the laboratory, the complexity of adjustment and operation with such a microscope, the need to control the microscope probe geometry to determine the scattering cross-section of a SPP, and the presence of a strong background scattering signal from exciting laser radiation on the macroscopic (greater than micron size) parts of the base and probe microscope holder. In this regard, this method has only been successfully used in a limited number of laboratories.

In this paper, we propose a different approach to measuring SPP properties. The idea consists of the placement of a nanoobject with controlled geometry into the SPP field, using nanolithograpy to form the object on the surface of metal nanofilms. The SPP characteristics are measured in accordance with the far-field wave scattering (similar to the method of near-field microscopy). We should emphasise the main advantages of the proposed approach: the geometry of a nanostructure which acts as a probe is known; the geometry of such a nanostructure does not degrade over time (in contrast to the probe of a near-field microscope); such a nanostructure has no macroscopic parts (there are no holders and, therefore, no accompanying background scattering of exciting laser radiation); and there is no need for additional complicated equipment.

2. Samples and optical measurements

We have used two types of nanofilms: 200-nm-thick monocrystalline (111) gold nanofilms formed by epitaxial growth on mica (Phasis company, Switzerland), and 200-nm-thick polycrystalline silver films formed on a polycrystalline quartz surface using the thermal sputtering technique in a vacuum at a pressure of 10^{-7} mbar. Micro- and nanostructures were formed using an FEI Quanta 3D dual column microscope, which has a highly focused beam of Ga ions. Electron microscopy studies were performed using a JEOL scanning electron

P.N. Melentiev, V.I. Balykin Institute of Spectroscopy, Russian Academy of Sciences, ul. Fizicheskaya 5, Troitsk, 108840 Moscow, Russia; e-mail: melentiev@isan.troitsk.ru;
A.A.Kuzin Institute of Spectroscopy, Russian Academy of Sciences, ul. Fizicheskaya 5, Troitsk, 108840 Moscow, Russia; Moscow Institute of Physics and Technology (State University), Institutskii per. 9, 141700 Dolgoprudny, Moscow region, Russia

microscope. The formation and characterisation of samples were conducted in a Class 100 clean room.

Optical measurements were carried out using an inverted Nikon Ti/U microscope with a PhotonMax (Princeton Instruments) CCD camera. The source of laser radiation was a tunable Ti:sapphire laser, where a phase half-wave plate was placed at the output to control the laser radiation polarisation.

Figure 1 displays the electron microscope images of the basic elements of plasmon optics formed on a 200-nm-thick monocrystalline film of gold (111) using the ion lithography method: nanoslit, nanogroove, nanohole, and nanopit. These elements enable the design of various elements of plasmon optics [1–3, 28]. However, only two of the presented structures – nanogrooves and nanopits – can be used to ensure nondestructive measurements of SPP parameters because, as we show below, there are small SPP losses on these elements. The interaction of SPPs with nanogrooves has been considered in many papers [29–32], which demonstrate the possibility of its use as an effective lens, mirror, or SPP splitter. In particular, Liu et al. [30] theoretically showed that the interaction process of a SPP propagating along a metal film surface with a nanogroove consists of two main parts: the excitation of the waveguide MDM mode in a nanogroove and the interference of this waveguide mode with a SPP. It was shown that under the condition of excitation of the waveguide MDM mode, the magnitude of SPP scattering from a nanogroove may reach several tens of percents.

In this work, a nanogroove was used as a SPP detector, which, by definition, must introduce minimal perturbations into the propagation of SPPs. According to Ref. [30], we need to select such nanogroove parameters at which the waveguide MDM mode is not excited. In particular, at a nanogroove width of 100 nm and depth of 25 nm, a cutoff regime for the waveguide mode is implemented, i.e. the waveguide MDM mode is not excited in the groove. In this case, the coefficient of SPP scattering from the nanogroove is small, i.e. about 1%. In the case of a nanopit, the scattering coefficient is even smaller. Below, we describe how the use of these two elements makes it possible not only to visualise the SPP propagation along a metal nanofilm surface, but also to measure its basic parameters, namely, the propagation length and directivity.

An extremely important element of plasmon optics is the SPP source. The following ways of its formation are known:

the use of the near field of laser radiation under the condition of its total internal reflection [33, 34] and the relaxation of excited quantum objects located near a metal nanofilm [35, 36]. The most versatile, easy to use, and practically important is the method of SPP excitation resulting from the scattering of laser radiation from gratings or nanostructures [37, 38].

The use of periodically arranged nanostructures ensures a high efficiency of laser energy transmission into a SPP [39]. If an array of nanoslits with period Λ, formed on a metal nanofilm surface, is used for that purpose, the following condition must be satisfied for efficient SPP excitation [37]:

$$\mathrm{Re}(\boldsymbol{k}_{\mathrm{SPP}}) \approx (mG + k_0 n_{\mathrm{sub}}\sin\alpha)\boldsymbol{x} + (k_0 n_{\mathrm{sub}}\sin\beta)\boldsymbol{y}, \qquad (1)$$

where $\boldsymbol{k}_{\mathrm{SPP}}$ is the wave number of a SPP; $G = 2\pi/\Lambda$ is the modulus of the reciprocal lattice vector of nanoslits; α and β are the angles of incidence of an exciting wave in the substrate relative to x and y axes, respectively; $k_0 = \omega/c$ is the wave number in a vacuum; m is an integer; and n_{sub} is the substrate refractive index.

Nanogrooves. Figure 2a illustrates a scheme of recording a SPP excited by an array of nanoslits using a nanogroove. A circular nanogroove is formed around the array on which the SPP is scattered. Scattering from the nanogroove generates a source of radiation, localised on the metal nanofilm surface, which can be observed using an optical microscope. Thus, the transverse size of such a source is determined by only two parameters, i.e. the groove width and SPP beam width.

The implementation of this scheme is demonstrated in Fig. 2b, which displays an optical-microscope image of the formed SPP source. An array of fifteen cut-through nanoslits has a size of 12 μm×100 nm and is each surrounded by a nanogroove with a diameter of 200 μm. The period of nanoslits is $\Lambda = 780$ nm, and the width and depth of the nanogrooves are equal to 100 and 25 nm, respectively. The nanostructures are formed by a highly focused beam of Ga ions in the monocrystal film of gold (111) with a thickness of 200 nm (Phasis, Switzerland). Laser radiation was incident on the sample along the normal to the nanofilm plane. The laser radiation wavelength was about 810 nm. The laser beam diameter in the sample plane was equal to the largest size of the array and was formed by a long-focus lens.

As can be observed from Fig. 2b, if the polarisation direction of laser radiation is perpendicular to the nanoslits,
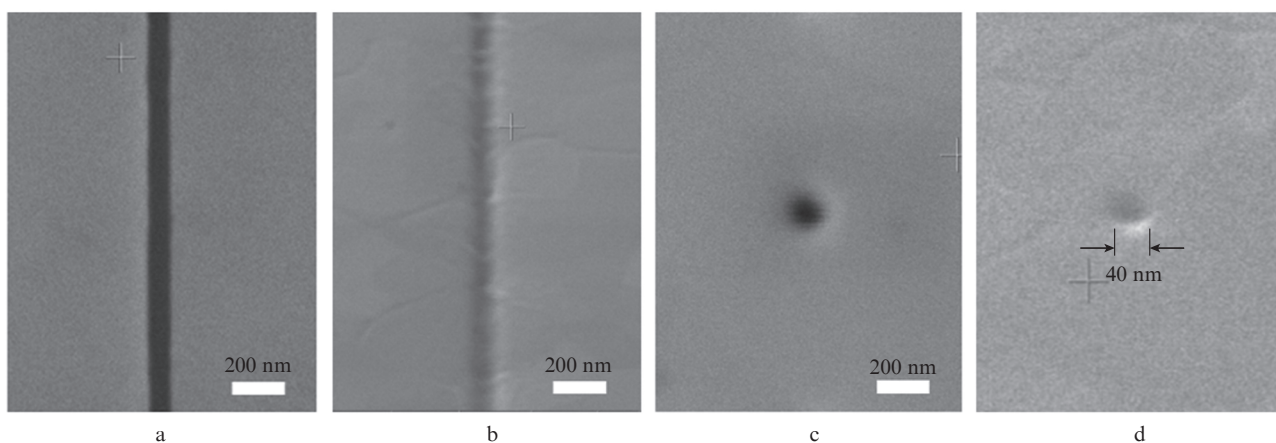

Figure 1. Basic elements of the plasmon optics manufactured in a monocrystalline film of gold (111) with a thickness of 200 nm: (a) nanoslit, (b) nanogroove, (c) nanohole and (d) nanopit.
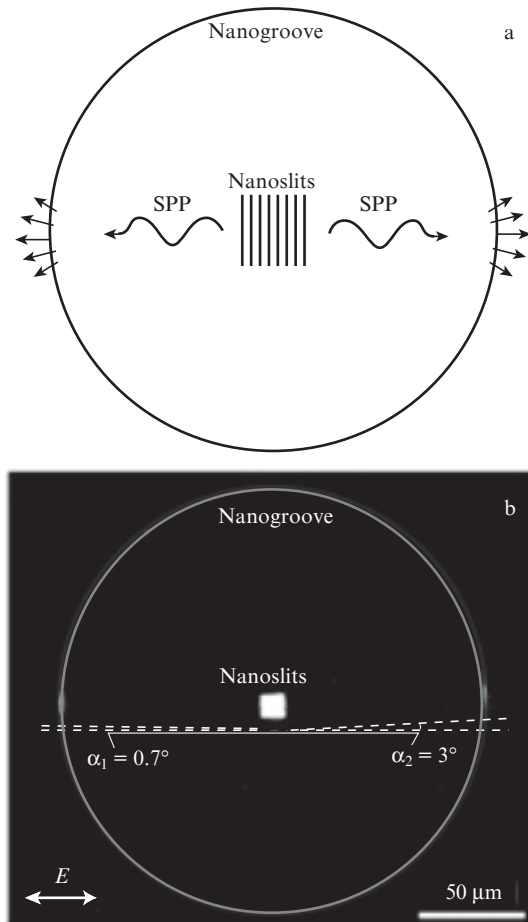
Figure 2. (a) Scheme of a plasmon wave source, which includes nanoslits formed in a metal nanofilm and circular nanogroove, on which the SPP is scattered. (b) Optical image of the SPP source implemented according to this scheme, provided the source is excited by laser radiation with a wavelength of 800 nm and polarisation direction is perpendicular to the nanoslits.

two bright radiation sources appear in the nanogroove region. (If the polarisation direction is orthogonal to the nanoslits, the radiation sources disappear.) The horizontal size of these sources is identical to that of a diffraction-limited spot of an optical microscope with a mounted lens of $20^{\times}$ (NA = 0.45). The vertical size of the source, determined by the SPP size at a distance of 100 μm, is 8 μm, which corresponds to the calculated values.

Figure 2b also indicates that the sources arising from the SPP scattering from a nanogroove are located at certain angles relative to the line perpendicular to the nanoslits. This is because the plasmon SPPs excited on the array of nanoslits are not located on one straight line because of the nonzero values of laser radiation angles of incidence on the substrate. The processing of experimental data shows that the angles α and β are equal to 0.7° and 3°, respectively.

Nanopits. Another nanostructure, which allows one to determine the SPP propagation parameters, is a nanopit (Fig. 1d). Figure 3 presents a sample image obtained using an optical microscope, which is similar to that shown in Fig. 2; the only difference is that the entire surface inside the circular nanogroove formed by ion lithography is filled with nanopits of 40 nm in diameter, 25 nm in depth, and a location period of 2 μm. The CCD-camera sensitivity was chosen to be quite

high to enable the experimental visualisation of SPP scattering from a single nanopit, which, in the case under consideration, forms a nanolocalised light source. It is observed that the SPP propagation is accompanied by the scattering from nanopits, which allows the direction of propagation to be traced and compared with the case of SPP scattering from nanopits.
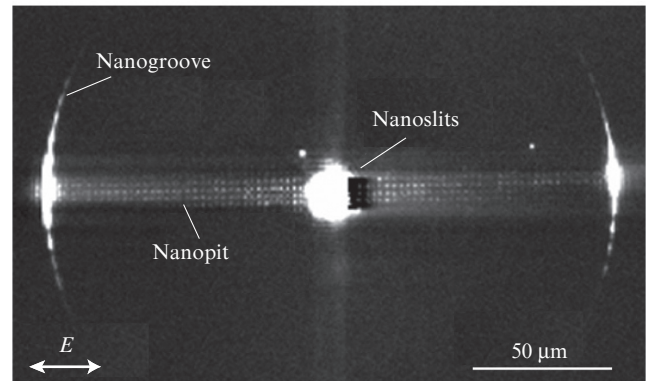

Figure 3. Optical image of a SPP source implemented in the form of nanoslits in the SPP recorded by nanopits and circular nanogrooves when excited by laser radiation (λ = 800 nm) with the field polarisation direction $\boldsymbol{E}$ perpendicular to the nanoslits.

As can be observed from Fig. 3, with the selected highly sensitive CCD camera, in addition to the radiation sources formed by nanopits, scattering characterised by a complicated periodic structure arises on a nanopit. The analysis of calculation data suggests that this is due to the diffraction of light from the nanoslits of finite length. We can observe an artefact caused by the CCD camera itself associated with the migration of charges between the adjacent camera pixels, which is especially apparent in the direction of the camera rows along which the charge flow occurs. To reduce the impact of this effect, the CCD camera was oriented so that its rows and, consequently, migration of charges, were orthogonal to the SPP propagation. As a result, one can see the traces of charge migration in the up and down directions from the array with nanoslits, which produces the brightest radiation source in Fig. 3; thus, the signal originating from the respective pixels of the CCD camera is brighter than the signal originating from the pixels that are not illuminated by light.

The measurement results on the propagation of plasmon waves using the nanopits are presented in Fig. 4. An optical image of an excited wave scattering from the nanopits formed in a silver film with a thickness of 200 nm is displayed in Fig. 4a. The parameters of the nanopits were chosen to be identical to those described above; the nanopits were positioned on the sample in the form of columns with a period of 66 μm, and the distance between the adjacent nanopits in a column was 15 μm. A SPP was excited by an array of nanoslits with a length of 200 μm and laser radiation (λ = 800 nm) illuminating a part of this array. The array slits were parallel to the nanopit columns. To avoid CCD-camera illumination by the light passing through the slits, the sample was positioned in the microscope in such a way that the array image was located outside the field of view of the CCD camera (to the left of the image presented in Fig. 4).

As can be observed from Fig. 4a, nanopits allow the visualisation of SSP propagation excited by laser radiation using
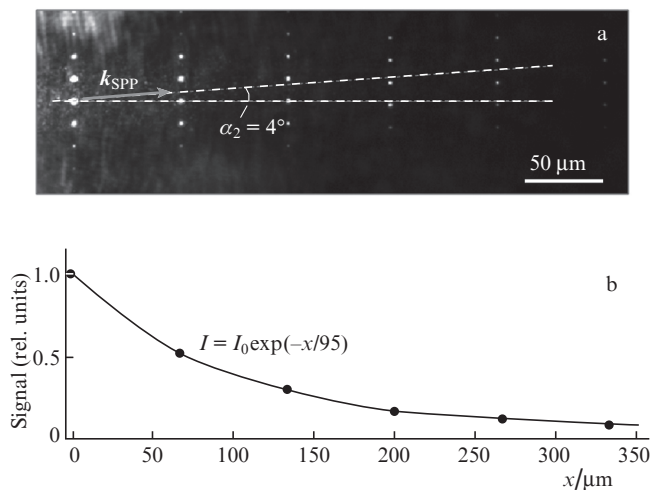
Figure 4. (a) Results of SPP propagation measurement using the nanopits: optical image of the excited wave scattering from the nanopits formed in a silver film with a thickness of 200 nm. (b) Dependence of intensity of SPP scattering from the nanopits on the distance between the nanopits and source.

an array of nanoslits. It is observed that because of the presence of small deviations in the laser radiation directivity from the normal to the sample, the SPP also propagates at a certain angle relative to the normal of the nanoslits and columns of nanopits. In this case, one can observe that the SPP decays as it propagates: the scattering amplitudes on the nanopits corresponding to different propagation lengths of SPPs vary greatly. Figure 4b presents the measured dependence of the scattering intensity of the propagating SPP on the distance between the nanopits and SPP source. It can be observed that the obtained decay dependence follows a decay function with an exponent of 95 µm quite well. Thus, the measurements based on the use of nanopits allow one not only to visualise the SPP track, but to also measure its propagation length.

A separate experiment was performed to determine the SPP losses on the nanostructures used for sensing the SPP field. With this aim in view, a sample was manufactured in which three SPP sources with identical geometries and different detectors were formed: with nanogrooves and nanoslits, with nanogrooves only, and with nanopits only. In the first case, we used the nanoslits which allow efficient SPP excitation using laser radiation with a wavelength of 800 nm (the parameters of slits are indicated in the caption to Fig. 2b). Seven nanogrooves were formed at 10 µm from each other parallel to the slits located on the silver film surface. Each nanogroove had a length of 100 µm, width of 100 nm, and depth of 25 nm. The nanopits were located between the nanogrooves at 2.5 µm from each other. In the second case, we used the same geometry of nanoslits and nanogrooves but without nanopits; in the third case, we used the same geometry of nanoslits and nanopits but without nanogrooves.

All three types of structures 'SPP source + detector' were excited by laser radiation with $\lambda = 800$ nm under identical conditions: normal incidence and polarisation direction orthogonal to nanoslits. A comparison between SPP scattering from the nanogrooves and nanopits in the three above-described samples allowed us to determine the SPP losses during scattering from a single nanopit and single nanogroove, and the efficiency of SPP excitation.

Thus, the measurements have indicated that the efficiency of SPP scattering from a single nanopit is small, i.e. it constitutes 0.02% of the intensity of a propagating SPP. In the case of a nanogroove, the efficiency amounts to 5%, which is much greater than the value found in the calculations of a paper [30]. The difference between our measurements and the calculations can apparently be attributed to the known ambiguity of the optical constants of metal nanofilms, which depend on the method of their manufacturing [40]. Knowing the efficiency of SPP scattering from a single nanogroove and assuming that there are no other critically important channels of SPP losses on a nanogroove, we are able to determine the efficiency of SPP excitation by a system of nanoslits. The efficiency of SPP excitation by laser radiation, which we have determined by means of this approach, amounted to 6.4% on both sides of the groove.

Focusing. Various methods of focusing are known in plasmons; the wave waist size at the focus point is measured using near-field microscopy [14] or leakage-radiation microscopy [13]. Figure 5 displays electron microscope images of nano- and microstructures, which allow the SPPs to be excited and focused. The SPPs are excited by illuminating a periodic structure through semi-circular nanoslits. The wave vector of excited SPPs, in this case, has a spatially nonuniform distribution: it is directed along the slit normal at the film points located near an extreme nanoslit. Therefore, during propagation, the SPP converges to a point, which is the geometric centre of the semicircles formed by the nanoslits.

In practice, the SPP in such a system is quite difficult to excite. Primarily, this is stipulated by the polarisation dependence of light transmission through the nanoslits, and, besides, by the engineering complexity of laser beam formation: the polarisation direction at each point of a nanoslit is orthogonal to the semi-circular nanoslits. This leads to the fact that, in practice, the efficiency of SPP excitation by means of linearly polarised laser radiation is different at each point of the nanoslit.

Figure 5b presents an optical image of the sample with nanoslits made in the silver film with a thickness of 200 nm; the inner radius of the system of nanoslits is 25 µm. In the assumed area of SPP focus (geometric centre of the semicircles formed by nanoslits), five nanogrooves with a length of 12 µm, width of 110 nm, depth of 25 nm, and distance between them of 2.2 µm are located. Figure 5c shows an optical image of the same sample when the matrix with nanoslits is illuminated by laser radiation with a wavelength of 800 nm, directed normally to the sample plane. The spot diameter of laser radiation was approximately 25 µm. The laser radiation polarisation is linear and its direction is orthogonal to the nanogrooves. It is noticed that in this case, an optical signal appears near the nanogrooves, corresponding to the scattering of the SPP excited on the nanoslits, which propagates toward the centre of the semicircles formed by the nanoslits. The scattering signal demonstrates the presence of the SPP caustic, which corresponds to SPPs focusing with a convergence angle of about 60°. The minimum size of the SPP waist is approximately 1 µm.

Note that the optical picture of the SPP focusing we have obtained is extremely sensitive to the parameters of exciting laser radiation: wavelength, incidence angle, and polarisation. This is explained by the fact that in accordance with equation (1), the efficiency of SPP excitation and the direction of its wave vector depend on these parameters.
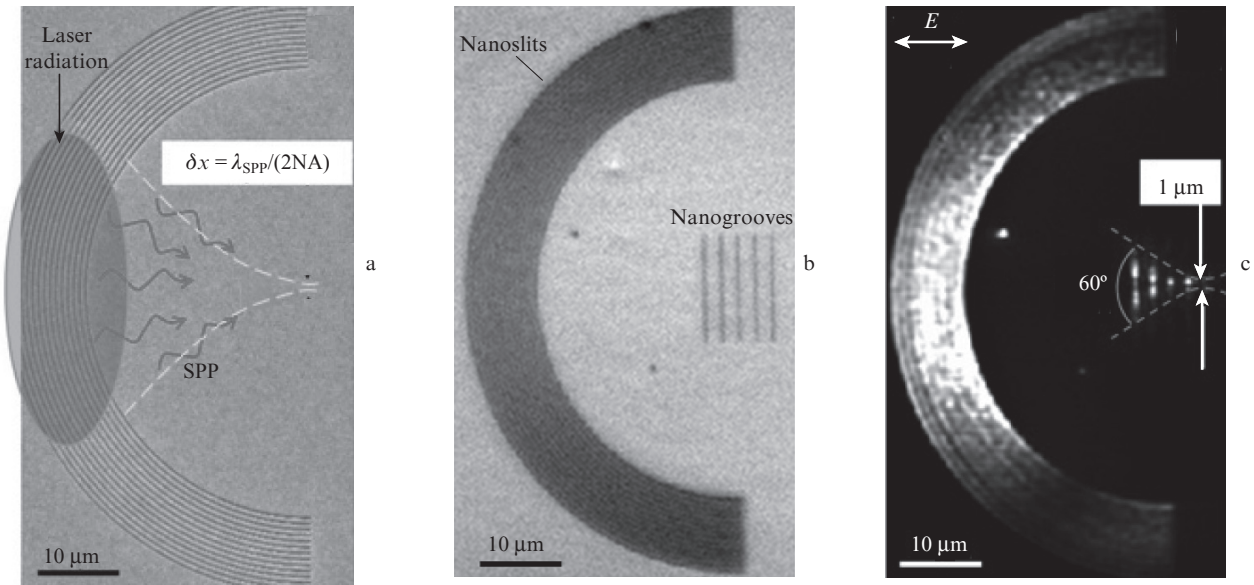
Figure 5. SPP focusing: (a) electron microscope image of semi-circular nanoslits formed in a silver film with a thickness of 200 nm when exciting the SPP by laser radiation; (b) optical image of the focusing element based on the nanoslits and detectors (nanogrooves) located in the focusing region in the absence of laser radiation; (c) optical image of the focusing element when irradiating the nanoslits by laser radiation with a wavelength of 800 nm orthogonally to the nanofilm, provided the polarisation direction is orthogonal to the nanogrooves.

The optical images of the sample under investigation obtained in the absence of a SPP (Fig. 5b) and its excitation (Fig. 5c) show the imperfections of the silver nanofilm surface: a through-hole, cavity, and structure in the form of a hillock arises in the process of nanofilm formation. The presence of such features of the nanofilm surface leads to losses in the excited SPP and its wavefront distortion. Figure 6 presents an optical image of the experimental sample being free of these disadvantages. A sequence of nanopits separated by 200 nm, acting as recording elements, is formed on the sample in the assumed area of SPP focusing. The image was acquired with the laser radiation parameters identical to those employed in the previous experiment.

As can be observed from Fig. 6, a bright spot corresponding to the scattering of the focused SPP from the nanopits appears in the focus area of the system of nanoslits. The spot cross-section along the line passing through the SPP focus area enables us to determine the spatial size of this region: 1 µm (see Fig. 5b).

Note that the focused signal intensity is four times greater than the local intensity of the SPP generated during the passage of laser radiation through the system of nanoslits. The measurements show that the SPP focusing allows a significant increase in the energy density of its electromagnetic field.

Thus, in the present work, we have experimentally demonstrated the possibility to control the properties of SPPs propagating along a metal nanofilm surface by scattering from nanoobjects – nanogrooves and nanopits – formed in the film. It is demonstrated that the use of such a technique makes it possible to measure the main parameters of SPPs.
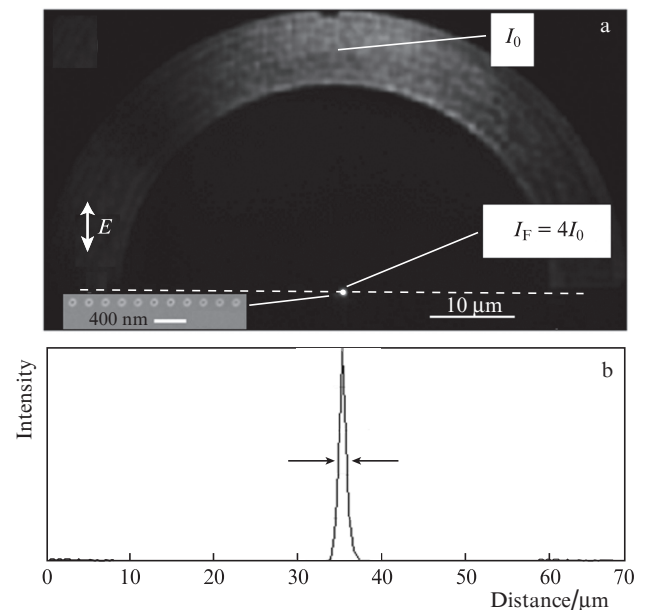
Figure 6. SPP focusing: (a) optical image of the focusing element (periodic array of semi-circular nanoslits) when irradiating the nanoslits by laser radiation ($\lambda = 780$ nm) orthogonally to a silver film (the nanopits with a diameter of 50 nm separated by 200 nm were used as detectors); (b) focusing area cross-section along the dashed lines, which indicates the spatial size of the plasmon wave focusing area (inset shows the photos of nanopits taken by an electron microscope).

References

1. Maier S.A. *Plasmonics: Fundamentals and Applications* (Springer Science & Business Media, 2007).
2. Klimov V.V. *Nanoplasmonics* (Singapore: Pan Stanford Publ., 2014).
3. Stockman M.I. *Opt. Espress*, **19**, 22029 (2011).
4. Atwater H.A. *Sci. Am.*, **296**, 56 (2007).
5. Brongersma M.L., Shalaev V.M. *Science*, **328**, 440 (2010).

6. Zia R., Schuller J.A., Chandran A., Brongersma M.L. *Mater. Today*, **9**, 20 (2006).

7. Kuttge M., García de Abajo F.J., Polman A. *Opt. Express*, **17**, 10385 (2009).

8. Oulton R.F., Pile D.F.P., Liu Y., Zhang X. *Phys. Rev. B*, **76**, 035408 (2007).

9. Ditlbacher H. et al. *Appl. Phys. Lett.*, **81**, 1762 (2002).

10. Krasavin A.V., Zayats A.V. *Appl. Phys. Lett.*, **90**, 211101 (2007).

11. Temnov V.V., Nelson K.A., Armelles G., Cebollada A., Thomay T., Leitenstorfer A., Bratschitsch R. *Opt. Express*, **17**, 8423 (2009).

12. Melentiev P.N., Kuzin A.A., Gritchenko A.S., Kalmykov A.S., Balykin V.I. *Opt. Commun.*, **382**, 509 (2017).

13. Radko I.P., Bozhevolnyi S.I., Brucoli G., Martín-Moreno L., García-Vidal F.J., Boltasseva A. *Opt. Express*, **17**, 7228 (2009).

14. Volkov V.S., Bozhevolnyi S.I., Rodrigo S.G., Martin-Moren L., García-Vidal F.J., Devaux E., Ebbesen T.W. *Nano Lett.*, **9**, 1278 (2009).

15. Homola J., Sinclair S.Y., Gauglitz G. *Sens. Actuators, B*, **54**, 3 (1999).

16. Byun Kyung Min, Sung June Kim, Donghyun Kim. *Appl. Opt.*, **46**, 5703 (2007).

17. Tong L., Wei H., Zhang S., Xu H. *Sensors*, **14**, 7959 (2014).

18. Homola J., in *Frontiers in Planar Lightwave Circuit Technology, NATO Science Series II: Mathematics, Physics, and Chemistry* (Dordrecht: Kluwer, 2006) Vol. 216, p. 101.

19. Raether H. *Surface Plasmons on Smooth Surfaces* (Berlin, Heidelberg: Springer 1988).

20. Balykin V.I., Melentiev P.N. *Usp. Fiz. Nauk*, in press (2017).

21. West P.R. et al. *Laser Photon. Rev.*, **4**, 795 (2010).

22. Boltasseva A., Atwater H.A. *Science*, **331**, 290 (2011).

23. Jer-Shing Huang et al. *Nature Commun.*, **1**, 150 (2010).

24. Melentiev P.N., Afanasiev A.E., Kuzin A.A., Gusev V.M., Kompanets O.N., Esenaliev R.O., Balykin V.I. *Nano Lett.*, **16**, 1138 (2016).

25. Dürig U., Pohl D.W., Rohner F. *J. Appl. Phys.*, **59**, 3318 (1986).

26. Betzig E.P.L.J.S., Finn P.L., Weiner J.S. *Appl. Phys. Lett.*, **60**, 2484 (1992).

27. Bozhevolnyi S.I., Smolyaninov I.I., Zayats A.V. *Phys. Rev. B*, **51**, 17916 (1995).

28. Barnes W.L., Dereux A., Ebbesen T.W. *Nature*, **424**, 824 (2003).

29. Kuttge M., Abajo F.J.G., de Polman A. *Opt. Express*, **17**, 10385 (2009).

30. Liu J.S.Q., White J.S., Fan S., Brongersma M.L. *Opt. Express*, **17**, 17837 (2009).

31. Lypez-Tejeira F. et al. *Nat. Phys.*, **3**, 324 (2007).

32. Liu J.S.Q. et al. *Nature Commun.*, **2**, 525 (2011).

33. Kretschmann E., Raether H. *Z. Naturforsch. A*, **23a**, 2135 (1968).

34. Otto A. *Z. Phys.*, **216**, 398 (1968).

35. Lakowicz J.R., Malicka J., Gryczynski I., Gryczynski Z. *Biochem. Biophys. Res. Commun.*, **307**, 435 (2003).

36. Zhang D., Fu Q., Yi M., et al. *Plasmonics*, **7**, 209 (2012).

37. Lopez-Tejeira F. et al. *Nature Phys.*, **3**, 324 (2007).

38. Renger J., Grafström S., Eng L.M. *Phys. Rev. B*, **76**, 045431 (2007).

39. Laluet J.-Y. et al. *Opt. Express*, **15**, 3488 (2007).

40. Kuznetsov S.M., Okatov M.A. *Spravochnik optika-tekhnologa* (Optical Technologist Handbook) (Leningrad: Mashinostroenie, 1983).